Two-dimensional Emission/Transmission Soot Concentration and Temperature Measurements†

Kevin Thomson[1,*], Matthew Johnson[2], Dave Snelling[1], Greg Smallwood[1]

[1]Combustion Group, Institute for Chemical Process & Environmental Tech., NRC

[2]Mechanical & Aerospace Engineering, Carleton University

Introduction

Soot emission from industrial combustors and engines has a major detrimental impact on air quality and human health, and is now being recognized as a key factor in global warming. Soot formation also plays an important role in the performance of these technologies. Reducing the environmental impact and improving operating efficiency of these devices are high priorities for most countries but can only be achieved with improved understanding of the fundaments of soot formation and oxidation.

Soot formation in flames is a complex process including a large number of different chemical species, inception and growth of particles in the nanometer range, and the agglomeration of small particles to larger aggregates [e.g., Haynes and Wagner, 1981; Bockhorn, 2000]. A number of kinetic models have been proposed during the last decades [Vlasov and Warnatz, 2002; D'Alessio et al., 1992; Frenklach, 2002; Krestinin, 2000], however, the mechanisms governing soot formation remain elusive. In the context of fundamental soot studies in steady laminar flames, line-of-sight attenuation (LOSA) and emission/transmission measurements remain a simple and valuable tool for spatially resolved measurement of soot concentration and temperature in single dimension or axi-symmetric flames.

Two dimensional LOSA (2D-LOSA) is a particularly attractive implementation of LOSA for soot formation studies in axi-symmetric flames [Snelling et al. 1999, Greenberg & Ku 1997]. In 2D-LOSA, a collimated beam of light is passed through a flame and imaged onto a CCD detector. Each pixel on the CCD represents a spatially independent measurement of the intensity of a portion of the collimated light beam after it passes through the flame. With a relatively simple analysis technique, it is possible to measure the entire soot concentration map of a flame. Thus researchers can rapidly characterize flames for various burner input parameters such as fuel type, additives, and input temperature. 2D LOSA suffers from limited sensitivity to low soot concentration and/or interferences due to beam steering induced by high temperature gradients in flames [Snelling et al. 1999]. To our knowledge no effort has been made to extending single wavelength emission/transmission diagnostic for determination of soot concentration and temperature as presented in [Hall & Bonczyk 1990] to a 2D form.

In this paper an alternative optical arrangement for 2D-LOSA referred to as Diffuse 2D-LOSA is presented which significantly improves the sensitivity of the diagnostic over [Snelling et al. 1999] by addressing the problem of beam steering interferences. This optical arrangement also allows for absolute light intensity calibrated two-dimensional soot emission measurements and thus allows rapid single wavelength two-dimension emission/transmission measurements of soot concentration and temperature from axi-symmetric flames.

Theory

Line-of-sight-attenuation (LOSA) is a well established optical method to measure soot concentration in an aerosol. In LOSA measurements, the transmissivity (propensity to attenuate light) of a soot aerosol is measured along a chord through the medium. The transmissivity of the chord, τ, at wavelength λ, measured by the ratio of light intensity before, $I_{\lambda,0}$, and after passing through the attenuating medium, I_λ, is functionally related to a line integral of the local extinction coefficients, $K_\lambda^{(e)}$, along the chord via:

$$\tau_\lambda = \frac{I_\lambda}{I_{\lambda,0}} = \exp\left(-\int_{-\infty}^{\infty} K_\lambda^{(e)} \mathrm{d}s\right) \qquad (1)$$

† Prepared for the 29th Task Leaders Meeting of the International Energy Agency Implementation Agreement on Energy, Conservation and Emissions Reduction in Combustion, Sub-task 3.4S, Gembloux, BE, September 2-6, 2007.

It is noted that soot concentration, f_v, relates to extinction coefficient as:

$$f_v = \frac{K_\lambda^{(e)} \lambda}{6\pi (1+\rho_{sa}) E(m)_\lambda}, \tag{2}$$

where $E(m)_\lambda$ is the soot absorption function and $\rho_{sa,\lambda}$ is the ratio of the scatter coefficient, $K_\lambda^{(s)}$, to the absorption coefficient, $K_\lambda^{(a)}$. For some aerosols, it is appropriate to assume that $\rho_{sa,\lambda} << 1$ and can therefore be ignored. In mediums where the soot concentration is not uniform, a single transmissivity measurement can only provide a measure of the average soot concentration along the chord. If, however, the soot field is axi-symmetric, measurements along multiple chords through the medium at a given cross-section combined with an inversion algorithm can be used to determine the local extinction coefficients, $K_\lambda^{(e)}(r)$, and thus radially resolved soot concentrations [Dasch 1992, Daun el al. 2006].

In an experimental setting, $I_{\lambda,0}$ and I_λ, are not measured directly. Instead, a transmissivity measurement is typically achieved by a sequence of four monochromatic measurements. The detected intensity of the lamp without the attenuation medium present (*lamp*), the intensity measured in the absence of lamp and attenuating medium (*dark*), the intensity with lamp and attenuating medium (*transmission*), and the intensity measured from the attenuating medium in the absence of the light (*emission*). The transmissivity is then calculated as:

$$\tau_\lambda = \frac{transmission - emission}{lamp - dark} \tag{3}$$

While soot emission is a bias which must be correctly removed from an attenuation measurement when measuring soot concentration, soot emission is used to advantage in measurement techniques such as two- or multi-wavelength pyrometry or emission/transmission measurement where soot concentration and temperature are both solved. In emission/transmission measurements, the soot extinction coefficient and soot concentration is solved from soot transmissivity measurements as described above while the soot temperature relates to the incandescent emission, denoted $G_\lambda(y)$ via:

$$G_\lambda(y) = \int_{-\infty}^{\infty} K_\lambda^{(a)}(x,y) B_\lambda\left[T(x,y)\right] \exp\left[-\int_x^\infty K_\lambda^{(e)}(x',y)\,dx'\right] dx \tag{4}$$

where $B_\lambda(T)$ is Planck's blackbody radiation function and the exponential term represents the effect of self-attenuation of soot incandescence as it propagates along the measurement chord. In order to solve for $T(r)$, eq. 4 must first be tomographically inverted. Unlike eq. 2, which can be expressed as the line integral of a property field [Hall & Bonczyk 1990] by taking the natural logarithm of $-\tau_\lambda$, eq. 4 is not a line integral of a property field because of the exponential term and is therefore not strictly invertible unless $-\int_x^\infty K_\lambda^{(e)}(x',y)\,dx' \approx 0$. In two- or multi-wavelength pyrometry this assumption is commonly made [e.g. Cignoli et al. 2001, Snelling et al. 2002]. With emission/transmission measurements, $K_\lambda^{(e)}(r)$ is known from transmission measurements and it is possible to apply a correction to the incandescence measurements before inversion. In this study, an approximate correction based on the Taylor series expansion of the exponential is used:

$$G_\lambda^{cor}(y) = \int_{-\infty}^{\infty} K_\lambda^{(a)}(x,y) B_\lambda\left[T(x,y)\right] dx = \frac{G_\lambda(y)}{1 + 0.5 \ln \tau(y)} \tag{5}$$

The corrected emission measurements do represent line integrals of a property field and can be inverted to find $K_{\lambda}^{(a)}(r)B_{\lambda}\left[T(r)\right]$ from which $T(r)$ can easily be solved since $K_{\lambda}^{(a)}(r)$ is known from the transmission measurements. Emission/transmission also offers advantage over two- or multi-wavelength pyrometry because knowledge of the spectral variation of the soot absorption function is not required.

Experimental Setup

The optical layout for Diffuse 2D-LOSA is included in Figure x. An arc lamp coupled with an integrating sphere produces a diffuse light source with a diameter of 25 mm. The output plane of the sphere is imaged to the centre of the particulate laden medium with a pair of optically conjugate achromatic lens (focal lengths 100 and 150 mm, diameters 50 mm) with a magnification of 1.5. The center of the medium is imaged onto a ccd detector using a second pair of optically conjugate lenses (focal lengths 508 mm, diameters 57 mm, apertured to 12.5 mm diameter) with 1:1 magnification. The 16 bit A/D CCD is filtered with NG filters and a 450 nm narrow bandpass filter.

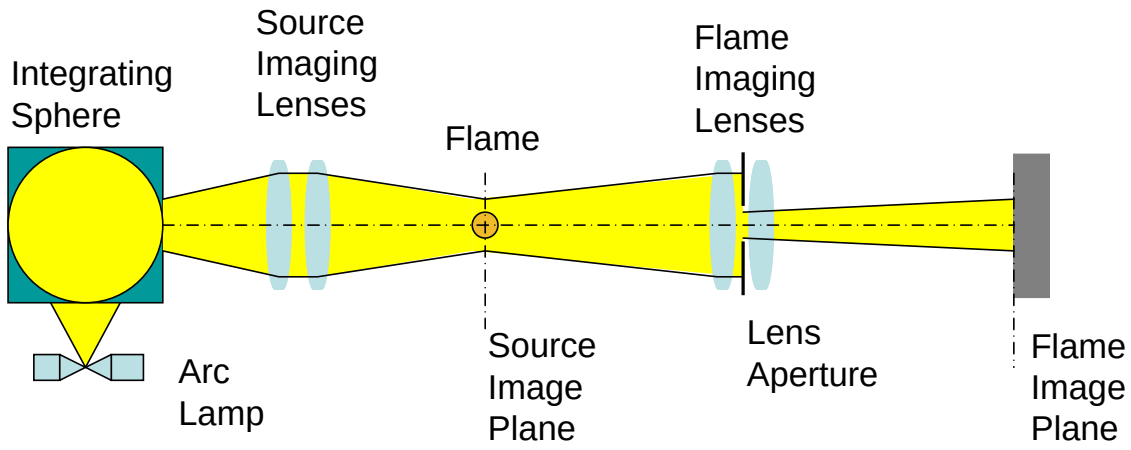

Figure 1 – Experimental layout of Diffuse 2D LOSA diagnostic

As part of the 2D emission/transmission diagnostic, the CCD must be calibrated across the field-of-view of the detector in terms of absolute light intensity collection efficiency at the measurement wavelength of 450 nm. This calibration is achieved using a spectrally calibrated radiance light source in the form of a lamp coupled to an integrating sphere with a 40 mm output window. The variation of the radiance output through the output port is specified to be less than 1%, thus providing an excellent calibration source for the 2D field. The sphere output port is located coincident with the source image plane or center of the particulate medium as shown in Figure 2.

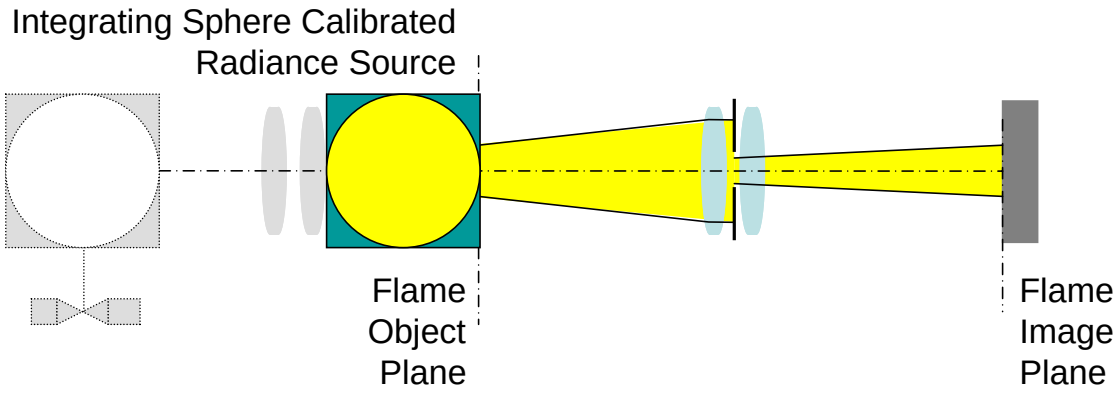

Figure 2 – Experimental layout for absolute light intensity calibration of CCD detector

A typical set of 2D emission/transmission images is included in Figure 3. It is noted that *emission* is required as part of the transmissivity measurement and so no extra measurements are needed for 2D emission/transmission as compared to 2D-LOSA. The images are binned horizontally (100 μm) and vertically (500 μm) to reduce shot noise. Horizontal sections of the transmissivity and emission are processed and inverted to determine the spatially resolved soot volume fraction and temperature. Samples of horizontal sections are included in Figure 4. Good symmetry is observed and very little noise. However, both the line-integrated extinction coefficients and emission measurements exhibit non-zero values on the outside edges of the soot envelope (i.e. +/- 5 mm) which might be indicative of 450 nm chemiluminescence interference in the soot measurement and/or image distortion due to optics limitations and/or beam steering.

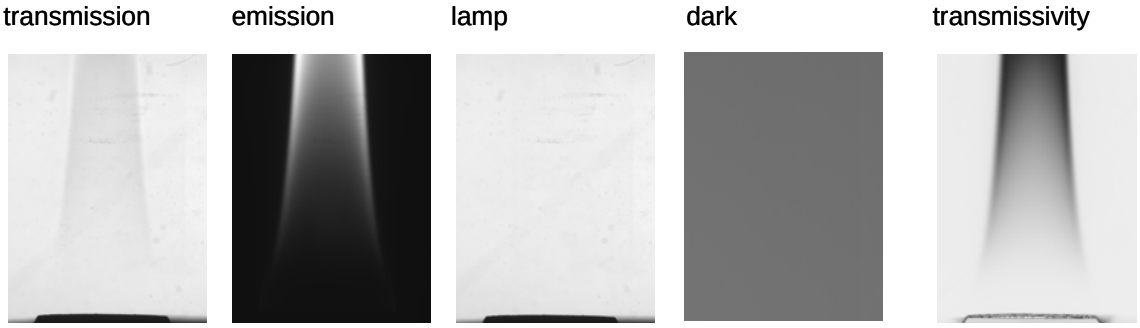

Figure 3 – 25 shot average images collected for an co-annular ethylene/air non-premixed Gulder burner flame (ethylene 194 sccm, air 284 slpm). *NB* image contrast optimized for each image.

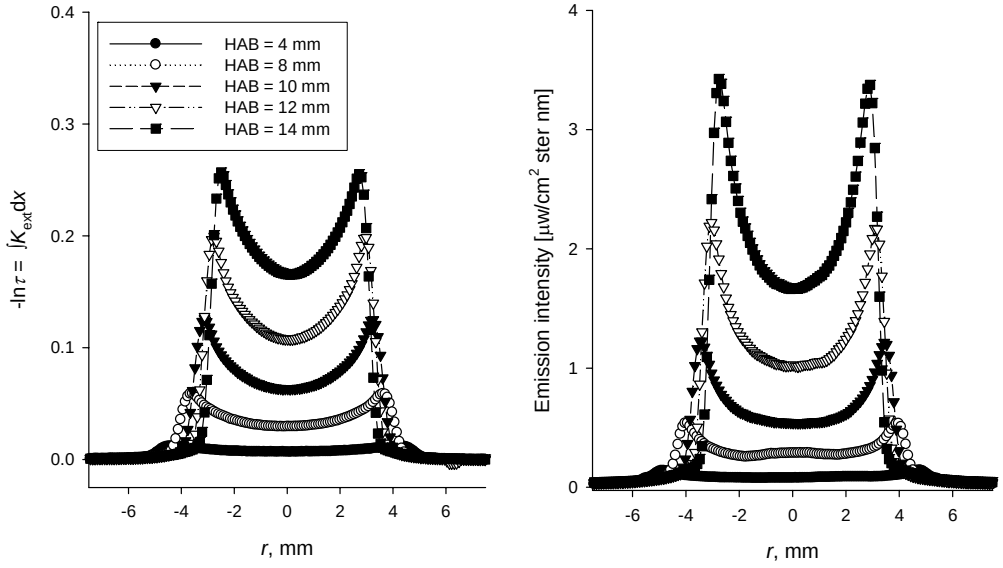

Figure 4 – Horizontal chords of a.) optical thickness $\left(-\ln\left(\tau_\lambda\right)=\int_{-\infty}^{\infty} K_\lambda^{(e)}\mathrm{d}s\right)$ and b.) flame emission at 450 nm.

Figure 5 includes contour plots of the f_v determined using traditional (collimated) 2D LOSA as outlined in [Snelling 1999] and f_v and T as measured here using 2D emission/transmission (diffuse LOSA). The two measurements of f_v are highly similar with slightly higher noise in the traditional 2D LOSA results. The temperature measurements have been filtered to zones where the soot volume fraction is above 0.5 ppm. Outside of this boundary, the temperature results are erratic due to low signal-to-noise and also possibly because of the problems with image quality observed in the emission image. A consequence of the filtering is that the range of observed temperature [1550 – 1800 K] is relatively small.

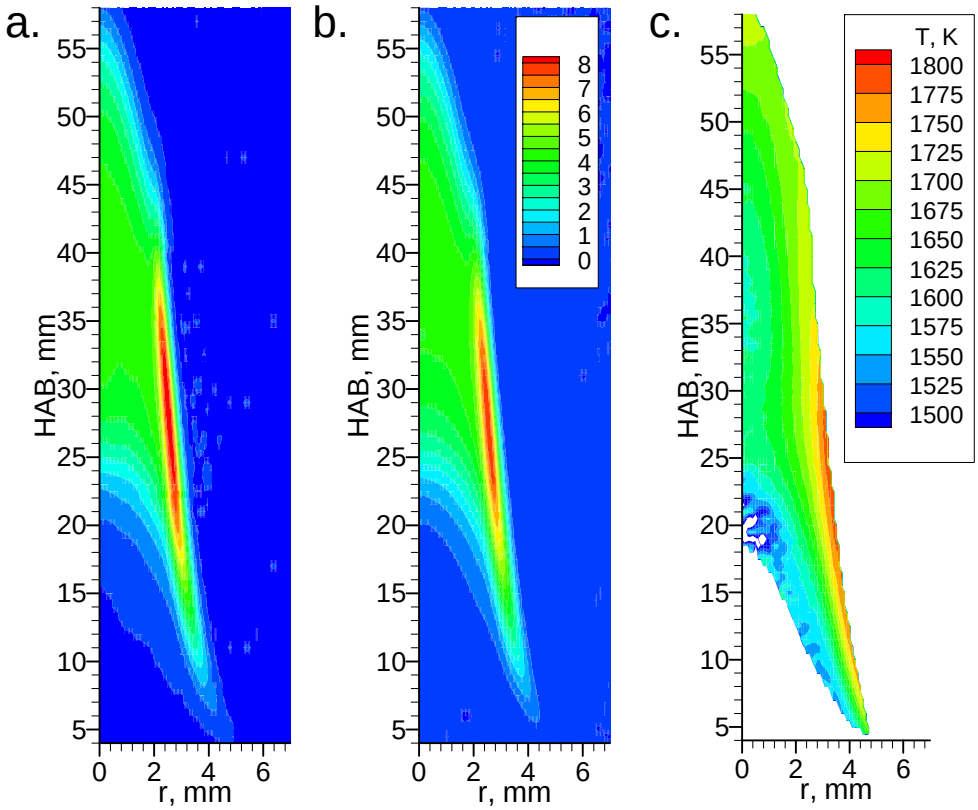

Figure 5 – a.) f_v [ppm] using traditional (collimated) 2D LOSA [Snelling et al. 1999], b.) f_v [ppm] with 2D emission/transmission (diffuse LOSA), c.) T [K] with 2D emission/transmission.

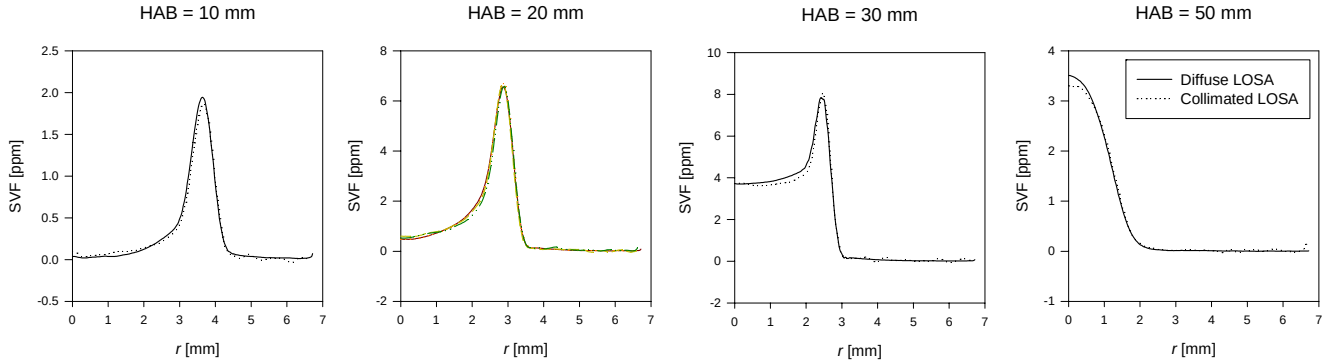

Figure 6 – f_v [ppm] using traditional (collimated) 2D LOSA [Snelling 1999] and 2D emission/transmission (diffuse LOSA) for selected HAB.

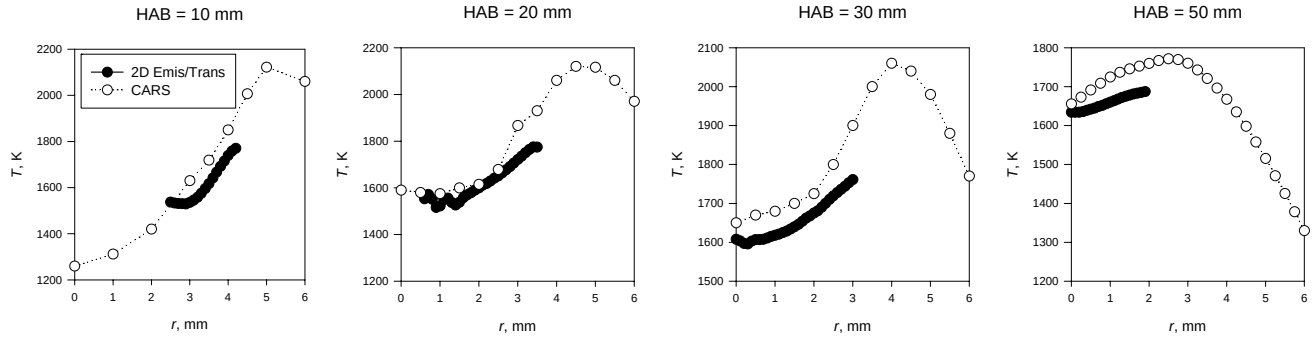

Figure 7 – T [K] using CARS [Snelling et al. 2002] and 2D emission/transmission (diffuse LOSA) for selected HAB.

A closer examination of the soot volume fraction is given in Figure 6. It is evident that the agreement between the traditional (collimated) 2D LOSA and this diffuse light based 2D transmissivity measurement are excellent. A comparison of the measured temperature with CARS based temperature measurements [Snelling et al. 1999] is shown in Figure 7. The agreement is quite good (typically better than 75 K) with the CARS temperatures consistently above the emission/transmission temperatures.

Conclusions

A 2D emission/transmission diagnostic is demonstrated which allows rapid characterization of soot concentration and temperature from axi-symmetric flames. The diagnostic provides excellent agreement with collimated 2D LOSA measurements of soot concentration and good agreement with CARS measurements of flame temperature. The temperature measurements are limited to regions there is good emission signal. Future work will include extension of the diagnostics to different wavelengths.

References

Bockhorn, H., 2000, "Ultrafine particles from combustion sources: approaches to what we want to know", *Phil. Trans. R. Soc. Lond*. A, **358**, pp. 2659-2672.

Cignoli, F, De Iuliis, S., Manta, V., and Zizak, G. 2001, "Two-dimensional two-wavelength emission technique for soot diagnostics," Applied Optics, vol. 40(30), p.5370-5378.

D'Alessio, A., D'Anna, A., D'Orsi, A., Minutolo, P., Barbella, R., and Ciajolo, A., 1992, "Precursor formation and soot inception in premixed ethylene flames," *Proc. Combust. Inst.*, **24**, p. 973.

Dasch, C. J. 1992, "One-Dimensional Tomography: A Comparison of Abel, Onion-Peeling, and Filtered Backprojection Methods," Applied Optics, Vol. 31(8), pp. 1146–1152.

Frenklach, M., 2002, "Reaction mechanism of soot formation in flames," *Phys. Chem. Chem. Phys.*, **4**, pp. 2028-2037.

K. Daun, K. Thomson, F. Liu, G. Smallwood 2006, "Deconvolution of axisymmetric flame properties using Tikhonov regularization," Applied Optics, vol. 45(19), p4638-4646.

Greenberg, P. S., Ku, J. C., „Soot Volume Fraction Imaging", Applied Optics, vol. 36(22), p5514-5522

Hall & Bonczyk 1990, "Sooting Flame Thermometry Using Emission/Absorption Tomography", Ap. Op., v.29, p. 4590–4598

Haynes, B. S. and Wagner, H. Gg., 1981, "Soot formation," *Prog. Energ. Combust.* **7**, pp. 229-273.

Krestinin, A. V., 2000, "Detailed modeling of soot formation in hydrocarbon pyrolysis," *Combust. Flame*, **121**, pp. 513-524.

D. Snelling, K. Thomson, G. Smallwood, and Ö. Gülder 1999, "Two-dimensional imaging of soot volume fraction in laminar diffusion flames," Applied Optics, vol. 28(12), p2478-2485.

D. Snelling, K. Thomson, G. Smallwood, Ö. Gülder, E. Weckman, R. Fraser 2002, "Spectrally resolved measurement of flame radiation to determine soot temperature and concentration," AIAA Journal, vol. 40(9), p1789-1795.

Vlasov, P. A. and Warnatz, J., 2002, "Detailed kinetic modeling of soot formation in hydrocarbon pyrolysis behind shock waves," *Proc. Combust. Inst*., **29**, pp. 2335-2341.